High-finesse disk microcavity based on a circular Bragg reflector

D. Labilloy,[a] H. Benisty, and C. Weisbuch
Laboratoire de Physique de la Matière Condensée, Ecole Polytechnique, URA 1254 CNRS, 91128, Palaiseau Cedex, France

T. F. Krauss and C. J. M. Smith
Department of Electronics and Electrical Engineering, Glasgow University, G12 8LT Glasgow, United Kingdom

R. Houdré and U. Oesterle
Institut de Micro et Opto-électronique, Ecole Polytechnique Fédérale de Lausanne, CH-1015 Lausanne, Switzerland

(Received 24 March 1998; accepted for publication 6 July 1998)

We made disk-shaped microcavities of approximately 10 μm^2 in area in a GaAs/AlGaAs waveguide structure by etching deep vertical concentric trenches. The trenches form a circular Bragg-like reflector that confines light in the remaining two lateral dimensions. We demonstrate from photoluminescence excited in the waveguide the confinement of discrete disk modes whose wave vector is mainly radial, in contrast with whispering gallery modes. Their quality factors up to $Q=650$ indicate in-plane reflectivities approaching 90%. In the near infrared, this represents a demonstration of wavelength-scale light confinement based on photonic crystal effects in two dimensions. © *1998 American Institute of Physics.* [S0003-6951(98)00336-2]

Light confinement at wavelength scale in semiconductor microcavities has been productive in controlling optical processes along the ''vertical'' growth axis of the semiconductor heterostructure.[1] Lateral light confinement at a similar scale is also desirable to control in-plane spontaneous emission.[2] Because in many devices this emission couples into the guided mode(s) of the heterostructure, adding lateral confinement in the two ''horizontal'' dimensions results in a resonator with discrete photon modes which are confined in three dimensions. Flat circular disks defined in a waveguide are the simplest realization of such resonators: Since the vertical k component is dictated by the waveguide, in-plane propagation may simply be accounted for by the use of an effective index n_{eff}.[3,4] Using, for simplicity, the crude zero-field boundary condition, the eigenmodes for a disk of radius R have the reduced vacuum wavelength $(\lambda_{m,n}/R)=2\pi n_{\mathrm{eff}}(\lambda_{m,n})/x_{m,n}$, where m and n are the azimuthal and radial quantum numbers, respectively, and $x_{m,n}$ is the nth zero of the mth Bessel function $J_m(x)$, whose first-order approximation is $x_{m,n}\approx(2n+m-1/2)\pi/2=\beta_{2m+n}$ for $m\ll n$.[5] Two noticeable kinds of modes are quasiradial modes [QRMs, Fig. 1(a), $m\ll n$] and whispering-gallery modes [WGMs, Fig. 1(b), $m\gg n$].[3,4] WGMs correspond to rays at almost grazing incidence that sample only the periphery of the disk. Their wave vector $\mathbf{k}$ is essentially tangential, $k_\varphi\approx k$. Conversely, rays of QRMs impinge close to normal incidence ($k_\varphi\ll k$). Because QRMs do sample the entire disk, controlling them is a key to improving the light–matter interaction in actual devices.

At present, there have been numerous successful realizations of microdisks sustaining high finesse WGMs,[4] on account of the good properties of total internal reflection (TIR) at grazing incidence. In contrast, reflectors that confine QRMs on a wavelength scale have not, to our knowledge, been demonstrated as yet. The shallow circular concentric gratings employed to define DBR-type (distributed Bragg reflector) round laser resonators offer surface emission capabilities,[6] but with useful modes of diameter ~100 μm. Conversely, at the wavelength scale, in-plane reflecting action of deep-etched straight trenches was demonstrated to provide lateral confinement in one dimension in micron-sized cavities around $\lambda=900$ nm.[7,8] In this letter, we combine these two approaches and study disk-shaped microcavities bounded by reflectors made of circular concentric deep-etched trenches [''leeks,'' Fig. 2(a)] in order to achieve more control of lateral spontaneous emission. The photonic band-gap approach inspired this photonic structure as well as that of Ref. 8. Here, we included emitters in the cavity that consist of self-organized InAs quantum dots (QDs).[9] Using their photoluminescence (PL), we demonstrate that our reflectors of inner diameter ~3 μm strongly confine the QRMs with low m values ($m\leqslant 9$).

A micrograph of a disk is shown in Fig. 2(b). The basic planar structure is a 0.24-μm-thick GaAs waveguide core

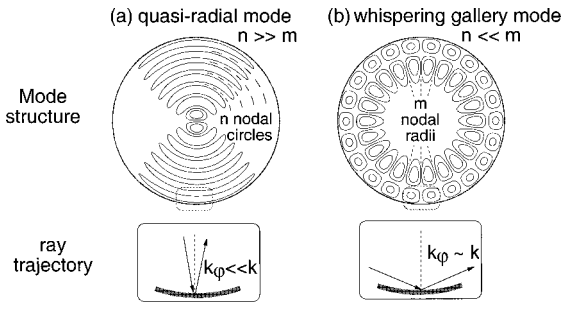

FIG. 1. Mode structure (top), and corresponding schematic ray trajectory (bottom), of (a) quasiradial modes and (b) whispering gallery modes; n and m are the radial and azimutal mode quantum numbers and k_φ is the ortho-radial k component.

[a]Electronic mail: dl@pmc.polytechnique.fr

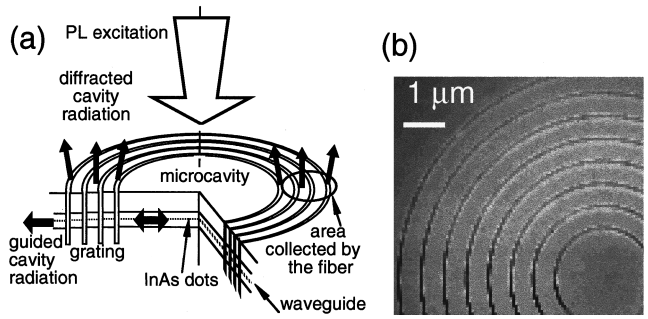

FIG. 2. (a) Schematic of the microcavity with circular trenches and measurement of resonances through localized detection of air-diffracted PL; (b) micrograph of a typical disk.

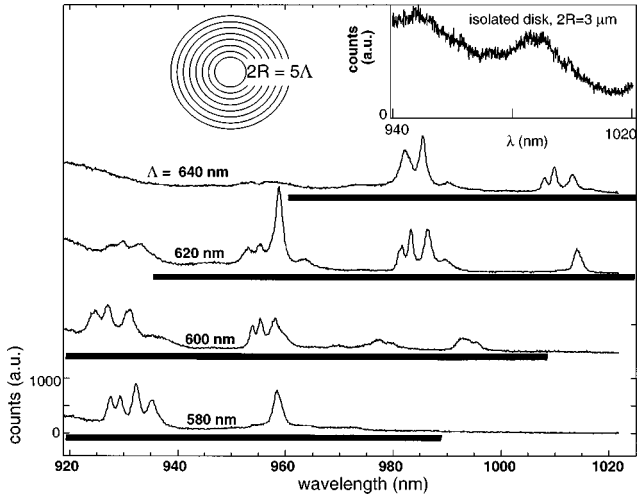

FIG. 3. Raw spectra of light collected selectively on the grating area of disks with pitches $\Lambda = 580$, 600, 620, and 640 nm, and diameters $2R = 5\Lambda$, with a vertical shift for clarity; stop bands of the grating are represented as dark bars below each curve. Inset: spectrum of stray light from an isolated disk of diameter $2R = 3\ \mu$m showing only smooth features.

embedding three layers of self-organized InAs dots.[9] A 0.34-μm-thick layer forms the top cladding. The circular trenches are deeply etched down to a depth $w \sim 0.8\ \mu$m in order to thoroughly cross the waveguide. The nanometer-scale e-beam lithography and etching methods are detailed in Refs. 10 and 11. The inner diameter of the disks is $2R = 2.9-3.2\ \mu$m, the concentric gratings consist of eight trenches of typical widths $t = 70$ nm and pitches $\Lambda = 580-640$ nm. These in-plane mirrors operate at the fourth Bragg order around $\lambda = 1\ \mu$m ($\Lambda = 4 \times [\lambda / 2n_{\text{eff}}]$ for $\lambda \sim 1\ \mu$m), given that $n_{\text{eff}}(\lambda) \approx 3.36 - 8 \times 10^{-4}[\lambda(\text{nm}) - 1000]$. The value of t is a compromise that ensures guided light reflection within a short length while minimizing out-of-plane scattering.[7,8]

Inside these resonators, we excite the QD photoluminescence in order for the guided spontaneous emission to probe the disk resonances. The dots offer the advantage of trapping the radiating electron-hole pairs, thereby reducing carrier diffusion towards etched interfaces and ensuring a large PL signal inside the disks. Furthermore, the deliberate broad distribution in dot size translates into a broad PL spectrum from 920 nm to well beyond our present 1040 nm detection limit. Photoexcitation is provided by a 678 nm laser diode beam focused to a $\sim 2\ \mu$m spot with a $\times 50$, NA$=0.50$ objective also used for PL collection. Next, a fiber located in the image plane of the objective feeds the collected signal to a spectrometer so as to perform localized PL (μ-PL) with a resolution $d \gtrsim 1\ \mu$m.[12]

Excited cavity modes are primarily outcoupled in the guided mode outside the disk, forming a beam awkward to collect [Fig. 2(a)]. The grating, however, provides backreflection through its fourth Bragg order (8π phase difference on a round trip between trenches), so successive rays diffracted towards the vertical axis have a 4π phase difference and, similarly to the surface emission mechanism of second-order DBRs,[6] guided light may be coherently outcoupled towards substrate and air [Fig. 2(a)]. Out of the two guided wave polarizations, TE and TM, only the first gives rise to a noticeable air emission because (i) at the source, the QD emit quite more in TE waves; (ii) in the grating, the TM diffraction efficiency vanishes around the vertical direction since in the regime $t \ll \lambda$, each trench acts as a punctual secondary source of radiation, akin to a vertical oscillating dipole in the TM case that does not radiate vertically. Even in the TE case, we estimate that not more than a few percents of the guided power is diffracted outside the guide per trench. Eventually, with the μ-PL setup collecting selectively light from the grating area, we do detect the horizontal TE disk resonances, with provisions detailed below. This ability to probe disk modes along the vertical axis greatly eases the test of a large number of disks. But conversely, from the resonator viewpoint, this diffraction represents a loss that reduces the grating reflectivity and/or its in-plane transmission.

On the same wafer, we etched a series of homothetic structures with pitches $\Lambda = 580$, 600, 620, and 640 nm and inner diameters $2R = 5\Lambda$. Our main observation is that many sharp peaks of width $\Delta\lambda = 1.5-5$ nm (hence quality factors up to $Q = 650$) show up on spectra collected from the grating area (Fig. 3), while light collected in the center exhibits no new features, or at most a minute remnant of the peaks. Peaks appear in clusters of one to four, but these clusters disappear at long wavelengths for $\Lambda = 580$ nm and at short wavelengths for $\Lambda = 640$ nm. They are separated by a free spectral range (FSR) of 27–33 nm typical of the disk diameter. As a crosscheck, we collected the stray light from the edge of an isolated disk without reflector ($2R = 3\ \mu$m) and found only broad modal features (inset of Fig. 3).

We, thus, attribute unambiguously these peaks to QRM resonances radiating in air through grating diffraction,[13] each cluster corresponding to a given value of $2n + m$, with successive odd and even clusters. Modes with higher m (from $m \sim 10$ up to WGMs) do not radiate in the grating region towards the objective or do not even radiate in air because of k conservation in Snell's law.[14]

These conclusions are first supported by the simple idea that one has to lie in the grating reflectivity stop band to build up sharp resonances. We calculated the position of these stop bands, using, for simplicity, a one-dimensional multilayer model in the case of normal incidence: we take a refractive index of unity for the thin trenches and the value $n_{\text{eff}}(\lambda)$ for the semiconductor ridges. The resulting stop bands are shown as black bars under each of the four curves in Fig. 3. The sharpest multiple clusters are located in the stop bands, while there are almost no marked features outside them. In detail, the long wavelength side of the stop band

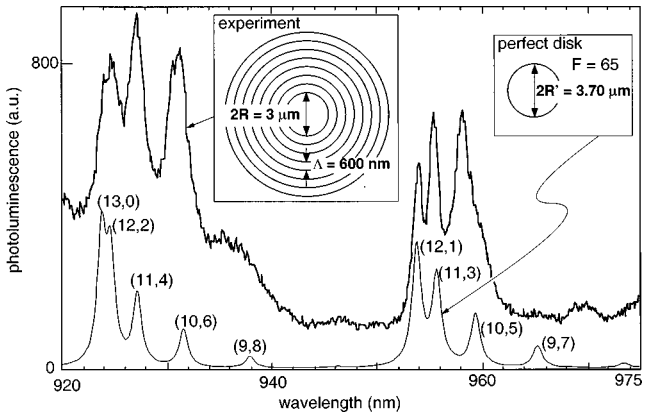

FIG. 4. Experimental data (upper curve) and simple disk model (bottom curve) for the $R=3\ \mu$m, $\Lambda=600$ nm structure. The finesse has been adjusted to 65 and the diameter to $2R'=3.70\ \mu$m. Numbers in parentheses are the mode numbers (m,n).

seems the worse, an effect which might stem from the oversimplified normal incidence assumption: it is well known that at oblique incidence, hence here for higher m values of QRMs, stop bands tend to shift to lower wavelengths.

Whereas a one-dimensional approach takes the effects of the grating periodicity into account, we shall neglect them in two dimensions in using a ''perfect disk'' model that focuses on those features that are specific to the round shape of the resonator: this model simply assumes a zero field at an effective diameter $2R'>2R$, in order to account for the field penetration depth into the circular grating. Resonant wavelengths of such a perfect disk are $\lambda_{m,n}=R'\times 2\pi n_{\rm eff}(\lambda)/x_{m,n}$,[5] for which we have the following expansion:[15]

$$\lambda_{m,n}\approx\frac{2\pi R n_{\rm eff}}{\beta_{2n+m}}\left(1+\frac{4m^2-1}{2\beta_{2n+m}^2}\right).$$

The first factor accounts for the succession of clusters associated to odd and even m number. Then, the fine structure within each cluster, given by m^2, is akin to the series (0,4,16,36,...) for even m but to the different series (1,9,25,...) for odd m. Next, the resonance widths result from the imperfect wall reflectivity, translating into a finite resonator finesse F, that we use as an estimate of the grating power reflectivity R_0 according to $F\approx 2\pi/(1-R_0)$. Finally, as m increases, light collection in air is impaired[14] and is expected to vanish for $m\sim 10$. We account for this effect through an *ad hoc* visibility factor $g(m)=\cos^2[(\pi/2)\times(m/10)]$ for $m\leqslant 10$, and $g(m)=0$ beyond, that does not modify the peak width. We hence calculate the intensity in this model as a sum of weighted Lorentzians $g(m)\times[1+(\lambda-\lambda_{n,m})^2/\Delta\lambda^2]^{-1}$, with a finesse $F=(\mathrm{FSR}/\Delta\lambda)$.

To fit the data of the 3 μm disk ($\Lambda=600$ nm), we use a finesse $F\approx 65$ (between clusters of same m parity and different n, i.e., with a $\sim$60 nm FSR) and an effective diameter $2R'=3.70\ \mu$m. We obtain the simulated spectrum of Fig. 4. The peak widths $\Delta\lambda$ are fairly well reproduced, as well as the typical alternate patterns from an even cluster (separations of about 1–3–5 nm, the two first peaks merging) to the next odd cluster (separations of about 2–4 nm). The strength of each peak within a cluster does not decrease as a function of m as it does in the simulation. The intrinsic or extrinsic (based on the measurement principle) nature of this discrepancy is still unclear to us. From the finesse, one concludes that the reflectivity at normal incidence is close to 90%.

In summary, by considering stop-bands and a simple disk model, we show clear evidence that the observed peaks stem from the quasiradial modes of the disk. Since confinement of QRMs cannot be achieved with TIR, our results clearly demonstrate the efficiency of the novel circular reflectors.

In conclusion, we demonstrate quasiradial microcavity modes in disks of diameter $\sim 3\ \mu$m bounded in two dimensions by a short circular grating and confined in a planar GaAs waveguide in the third dimension. These quasiradial modes are confined by the circular grating whose reflectivity may be as high as 90%, leading to a quality factor $Q\approx 650$. This grating is a novel solution for lateral light confinement and spontaneous emission control, going beyond the limitation of total internal reflection that confines only whispering-gallery modes and represents to our knowledge the first demonstration of photonic crystal effects in two dimensions of a microcavity.

The authors would like to thank Professor R. M. De La Rue and Dr. J.-M. Gérard for useful discussions. This work is supported by European Contract ESPRIT SMILED. One of the authors (C.J.M.S.) is supported by an EPSRC CASE award with BT Laboratories.

[1] *Optical Processes in Microcavities*, edited by R. K. Chang, and A. J. Campillo (World Scientific, Singapore, 1996).
[2] T. Baba, IEEE J. Sel. Top. Quantum Electron. **3**, 809 (1997).
[3] R. P. Wang and M.-M. Dumitrescu, J. Appl. Phys. **81**, 3391 (1997).
[4] R. E. Slusher and U. Mohideen, in Ref. 1, p. 315.
[5] B. E. A. Saleh and M. C. Teich, *Fundamental of Photonics* (Wiley, New York, 1991).
[6] A. A. Tovar and G. H. Clark, J. Opt. Soc. Am. A **14**, 3333 (1997), and references therein.
[7] T. F. Krauss and R. M. De La Rue, in *Photonic Band Gap Materials*, edited by C. M. Soukoulis (Kluwer, Dordrecht, 1996), p. 427.
[8] T. F. Krauss, B. Vogele, C. R. Stanley, and R. M. De La Rue, IEEE Photonics Technol. Lett. **9**, 176 (1997).
[9] J. M. Gérard, J. Y. Marzin, G. Zimmermann, A. Ponchet, O. Cabrol, D. Barrier, B. Jusserand, and B. Sermage, Solid-State Electron. **40**, 807 (1996).
[10] T. F. Krauss, R. M. De La Rue, and S. Brand, Nature (London) **383**, 699 (1996).
[11] D. Labilloy, H. Benisty, C. Weisbuch, T. F. Krauss, R. M. De La Rue, V. Bardinal, R. Houdré, U. Oesterle, D. Cassagne, and C. Jouanin, Phys. Rev. Lett. **79**, 4147 (1997).
[12] D. Labilloy, H. Benisty, C. Weisbuch, T. F. Krauss, R. Houdré, and U. Oesterle, Appl. Phys. Lett. **71**, 738 (1997).
[13] The dispersion of this grating is not a severe impairment. For normal incidence on the grating, the air beam angle $\theta(\lambda)$ is given, by $\sin\theta=n_{\rm eff}\times(\lambda-\lambda_0)/\lambda_0$, where λ_0 is the wavelength emerging at $\theta=0$. In our data $(\lambda-\lambda_0)/\lambda_0\sim 0.1$, so that $\sin\theta$ remains in the 0.5 collected aperture.
[14] The field of disk modes (m,n) contains $\exp(im\varphi)$ factors. Upon circulating by $L=2\pi r$ onto a loop of radius r, by matching $\exp(im2\pi)$ to the plane-wave form $\exp(ik_\varphi L)$, one finds $k_\varphi=m/r$; as a first-order estimate, Snell's law dictates the outside angle of incidence θ' of rays diffracted in air in the azimuthal direction according to $\sin\theta'=k_\varphi/k=\lambda m/2\pi r(k=2\pi/\lambda)$. At $\lambda=1\ \mu$m, for the typical value $r=2.5\ \mu$m of detection in the grating area, the air beam is allowed ($\sin\theta'\leqslant 1$) up to $m\approx 16$, while light collection ($\sin\theta'\leqslant 0.5$) holds only up to $m\approx 9$. Note that for WGMs, m is of the order of 50 ($m\lambda\approx 2\pi R n_{\rm eff}$).
[15] *Handbook of Mathematical Functions*, edited by M. Abramowitz and I. A. Stegun (Dover, New York, 1965).